HETEROCYCLES, Vol. 106, No. 10, 2023, pp. -. © 2023 The Japan Institute of Heterocyclic Chemistry
Received, 9th August, 2023, Accepted, 30th August, 2023, Published online, 7th September, 2023
DOI: 10.3987/COM-23-14895

A SERIES OF NOVEL COUMARIN DERIVATIVES: DESIGN, SYNTHESIS AND EVALUATION OF ANTI-TUMOR ACTIVITY

Zhuo Zhang, Bing He, Fei-Yang Shang, and Li-Qin He*

(These authors contributed equally: Zhuo Zhang and Bing He)

College of Pharmacy, Anhui University of Chinese Medicine, Hefei 230012, China;
E-mail: hlq661125@126.com

Abstract – A series of novel coumarin derivatives were synthesized and evaluated for their solubility and *in vitro* anti-proliferative activities against seven different tumor cell lines. As a result, most of the target compounds exhibited prominent inhibitory activities. Especially, compound **12c** exhibited the most potent inhibitory activity with IC_{50} values of 0.29-0.84 μM for both six tumor cell lines and one drug-resistant tumor cell line Bel-7402/5-FU, which are 5.45 - 22.55-fold better than 5-FU. Mechanism research revealed that compound **12c** blocked the cancer cell cycle at the G2/M phase and induced apoptosis of tumor cells. Our results indicate that compound **12c** is worth further investigating as an effective anti-cancer candidate.

INTRODUCTION

Cancer is one of the top killer diseases nowadays in the world. Liver cancer was the second leading cause of cancer death based on the WHO reported in 2020.[1] At present, there are many anti-cancer drugs in the clinic. However, most of the anti-cancer drugs are limited in clinics due to drug resistance and various side effects including peripheral neuropathy, alopecia, gastrointestinal reaction, infection, hemorrhage, erythra, etc.[2,3] Therefore, it is particularly necessary to develop some new anti-cancer agents with high efficiency, safe and low drug resistance. To date, natural products have attracted much attention due to diverse bioactive and low toxicity. There is a good strategy to develop novel anti-cancer agents using natural products as lead compounds.

As a kind of natural product, coumarins exhibit various biological activities such as anti-tumor,[4] anti-virus,[5] anti-bacteria,[6,7] nerve protection and anti-coagulation,[8,9] etc. In recent decades, it has attracted significant interest due to the various biological activities of coumarins. Some natural, semi-synthetic, and total synthetic lead molecules bearing coumarin scaffold have been discovered and applicated in anti-cancer

drug development.[10-15] For example, osthole (**A**, Figure 1),[16] a natural bearing coumarin scaffold, displayed moderate inhibition activity against three human hepatocarcinoma SK-HEP-1, SMMC-7721, HepG-2 cells and mice hepatocarcinoma Hepa1-6 cells with IC_{50} values of 137.0-189.5 μM. Psoralen (**B**, Figure 1), obviously displayed cytotoxicity against human breast cancer EMT6 cells *in vitro* and *in vivo*.[17] Therefore, the design of anti-cancer drug by introducing the coumarin scaffold would enhance the anti-cancer activity. Nitric oxide (NO), a kind of signal molecule, plays various roles in physiological functions including neuroprotective,[18] relaxation of smooth muscle,[19] inhibition of platelet aggregation,[20] regulation of blood pressure and induction of apoptosis, etc.[21,22] Notably, a high concentration of NO can induce apoptosis, inhibit metastasis of tumor cells, and increase the sensitivity of tumor cells to chemotherapy, radiation, and immune-therapy *in vitro* and *in vivo*.[23] As one class of NO donors, furoxans can produce high levels of NO *in vitro* and inhibit the growth of tumors *in vivo*. So, NO-releasing anti-cancer compounds often introduce the furoxan group to enhance their activity. Liu group designed and synthesized sixteen furoxan-based nitric oxides (NO) releasing coumarin derivatives.[24] The results found that **C** (Figure 1) exhibited the strongest anti-proliferation activity (IC_{50} = 0.014 μM) on the human ovarian carcinoma A2780 cell line. In addition, a large number of studies and reports further demonstrate that the modification of the coumarin skeleton will be beneficial to develop many novel anti-cancer drugs with better efficacy, high selectivity, and low side effects.[10-15]

In our previous study, we designed and synthesized a series of NO-donating coumarin-3-carboxylic acid derivatives.[25] As a result, we found compound **D** (Figure 1) showed the most antiproliferative activities on human breast MCF-7 cell (IC_{50} = 7.90 μM), human colon SW620 and HCT-116 cells (IC_{50} = 1.86 μM and 3.46 μM), human hepatocarcinoma HepG2 cell(IC_{50} = 9.85 μM) respectively. However, due to the low water solubility of **D** (4.81 mg/L), its application and development were limited. Thus, we modified the compound **D** to solve water solubility and increase the antitumor activity.

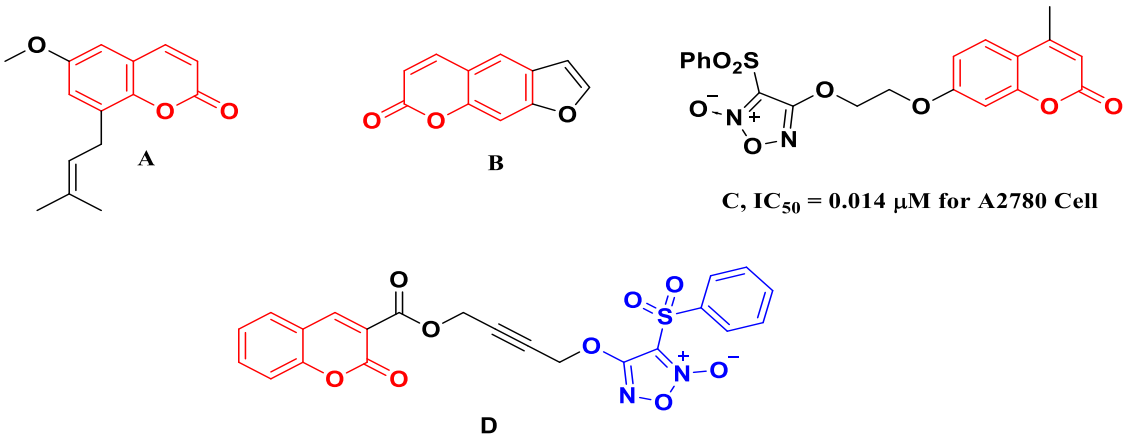

Figure 1. The structures of coumarin derivatives

By analyzing the structure of **D**, we found that introducing various hydrophilic organic amine moieties at the coumarin could improve water solubility. However, it is difficult to directly introduce these hydrophilic organic amine moieties at the coumarin. Considering all the above, we designed **D** analogs starting from 7-hydroxycoumarin-3-carboxylic acid by using the molecular hybridization approach (Figure 2). We previously synthesized many **D** analogs by introducing morpholine alkoxy groups with different chain lengths at the C7 position. As a result, we discovered 3C or 4C linker of **D** analogs showed strong inhibitory activity in human carcinoma cells.

Herein, a series of novel coumarin derivatives (Figure 2) bearing substituents at the C3 position of the furoxan moiety and at the C7 position of the hydrophilic organic amine moiety were designed and synthesized. Then, the anti-tumor bioactivity of these target compounds was evaluated and discussed. Furthermore, for the most potent compound *in vitro*, the anti-tumor activity in vivo and the potential to induce apoptosis and cell cycle arrest in human carcinoma cells were evaluated.

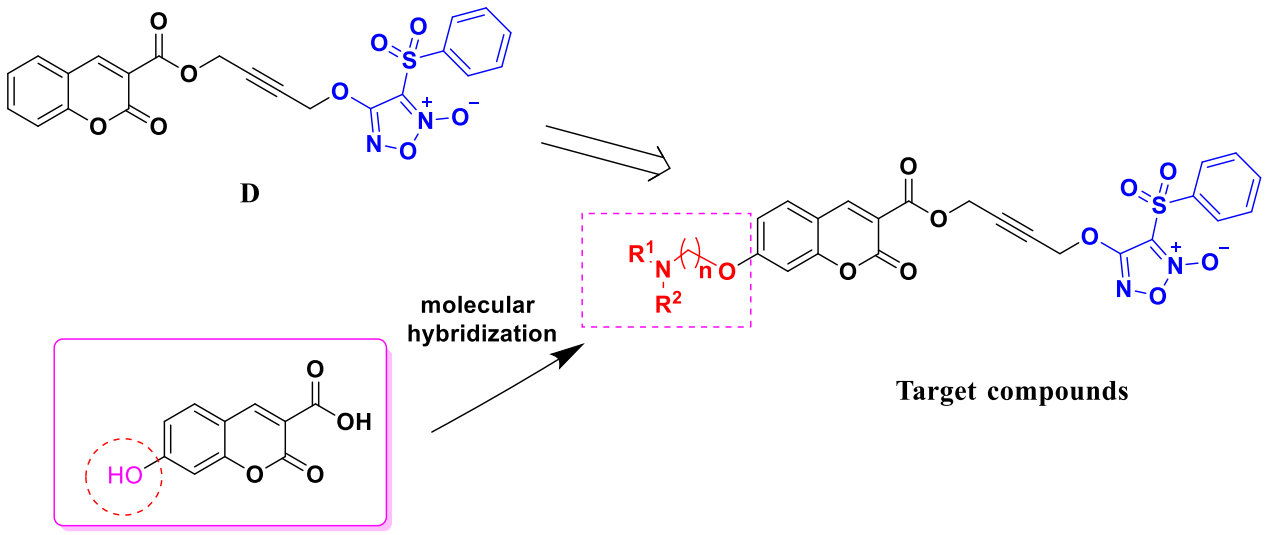

Figure 2. Design strategy of coumarin derivatives

RESULTS AND DISCUSSION

The synthetic route of target compounds is summarized in Schemes 1.

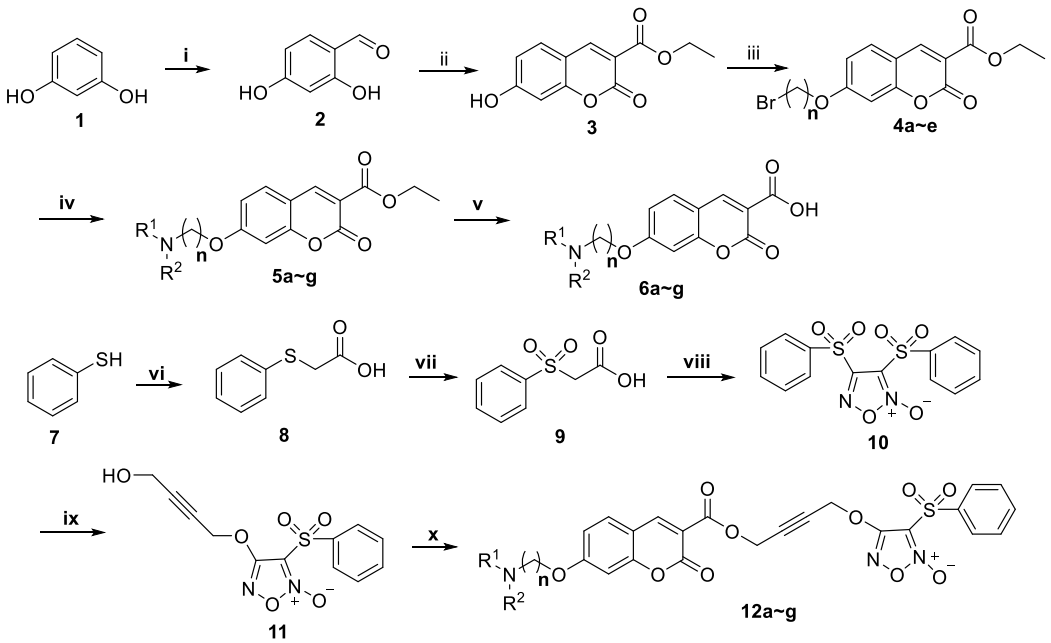

Scheme 1. Synthetic Routes of Target Compounds **12a-g**. Reaction conditions and reagents: (i) 1) DMF, $POCl_3$, MeCN, ~0 ℃, 6 h; 2) H_2O, $Na_2S_2O_3$, 50 ℃, 0.5 h; (ii) diethyl malonate, piperidine (cat.), HOAc (cat.), EtOH, reflux,10 h; (iii) Br-R-Br, DMF, K_2CO_3, 70 ℃, 1 h; (iv) DEA, morpholine, DMF, K_2CO_3, 70 ℃, 2 h; (v) 1) NaOH, H_2O, EtOH, 100 ℃, 20 min; 2) HCl, rt; (vi) NaOH, EtOH, H_2O, chloroacetic acid, Na_2CO_3, rt, 4 h and reflux 1 h; (vii) HOAc, H_2O_2, rt, 4 h; (viii) 98% HNO_3, reflux, 30 min; (ix) 1,4-butyne diol, THF, 25% NaOH, 0 ℃, 40 min; (x) Compound **6a-g**, DCM, DMAP, EDCI, TBAB, rt, 5 h.

Table 1. Structures of target compounds **12a-g**

Compd.	N	-NR^1R^2	Compd.	N	-NR^1R^2
12a	2	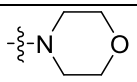	**12e**	6	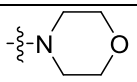
12b	3	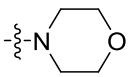	**12f**	3	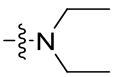
12c	4	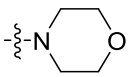	**12g**	4	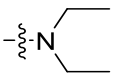
12d	5	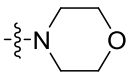			

The solubility test

To investigate whether enhance the solubility of these target compounds by introducing the different organic amine segments, the aqueous solubility was tested by UV method and cLogP was calculated by software SYBYL-X. As shown in Table 2, the aqueous solubility of these compounds was greatly improved compared to compound **D**. Among them, compound **12b** exhibited the highest

solubility with 13.84 mg/L compared to other target compounds. The aqueous solubility of compound **12c** also reached 13.05 mg/L. All cLogP were around 3, which indicate that the target compounds may have good permeability. The results indicate the improvement of solubility may relate to the introducing various hydrophilic aminoalkyl ether at the C7 position.

Table 2. The aqueous solubility and clogP of **12a-g**

Compd.	Solubility (mg/L)	cLogP
12a	13.52	2.3091
12b	13.84	2.6133
12c	13.05	2.7208
12d	12.62	3.2498
12e	12.23	3.7788
12f	13.59	3.2388
12g	11.24	3.1718
D	4.81	1.8330

***In vitro* cytotoxic activity of the target compounds**

The anti-proliferative effects of the target compounds were investigated in six different human cancer cell lines, including HeLa (human cervical cell line), SW620 and HCT-116 cells (human colon cell lines), MCF-7 (human breast cell line), HepG2 and Bel-7402 (human liver cell lines) and a normal human cell line, LO2 (human normal liver cell line) by MTT assay, using 5-FU as the positive control. The results were shown in Table 3. The target compounds showed different anti-proliferation activities against different tumor cell lines. For example, all compounds displayed strong anti-proliferation activity on HepG2 tumor cells. Conversely, for human cancer HeLa, SW620, HCT-116 and Bel-7402 cells, compounds **12a**,**12e-g** showed less cytotoxic activity with IC_{50} values more than 10 μM, but compounds **12b-d** exhibited higher cytotoxic activity stronger than the positive control drug 5-FU. Compounds **12b** and **12c** exhibited higher cytotoxic activity than the positive control drug in all tested cancer cell lines. In addition, compounds **12b-d** exhibited higher cytotoxic activity stronger than **D** for all tested cancer cells.

In addition, morpholino-containing compounds **12b** and **12c** exhibited better inhibitory activity against six different human cancer cell lines with IC_{50} values ranging from 0.29 – 0.84 μM, which are 5.45 - 22.55 fold better than that of **D** on HeLa, SW620, HepG2, HCT-116 and MCF-7 cell lines. Especially, **12c** exhibited the best inhibitory activity against the MCF-7 and HCT-116 cells, with an IC_{50} value of 0.29 μM and 0.48 μM respectively. Notable, the antiproliferative activity of

12c (IC_{50} = 0.33 μM) against Bel-7402 cells was 22.5-fold more than that of 5-FU, and against human normal liver cell LO2 with IC_{50} values of 1.07 μM. However, **12f** and **12g** showed the lowest inhibitory effect on HeLa, SW620, HCT-116, MCF-7, Bel-7402 cell lines, with the IC_{50} > 10 μM. It could decrease their activity due to introducing the diethylamine segments.

At present, the drug resistance and multidrug resistance of anticancer drugs become an awkward question in clinics. Drug resistance could severely affect the therapeutic effect. Therefore, the antiproliferative activity of compound **12c** against Bel-7402/5-FU cell was investigated. **12c** displayed high activity against 5-FU-resistant tumor cell line Bel-7402/5-FU with IC_{50} values of 0.63 μM. The results indicated that compound **12c** could inhibit the Bel-7402/5-FU. Thus, **12c** was selected to further investigate the mechanism as an anti-cancer candidate.

By analyzing the structure-activity relationship of **12a-g**, it was found that introducing morpholine ring could obviously enhance their anti-proliferative activity. The results indicated that the four-carbon chain at the C7 position directly connected to the morpholine ring was crucial for maintaining high potent activity.

Table 3. *In vitro* cytotoxic activity for target compounds against seven cancer cell lines and normal human liver cell line by MTT method

Compd.	IC_{50} (μM)							
	HeLa	**SW620**	**HepG2**	**HCT-116**	**MCF-7**	**Bel-7402**	**Bel-7402/5-FU**	**LO2**
12a	>10	>10	0.76±0.10	>10	1.05±0.35	>10	NT	NT
12b	0.47±0.20	0.56±0.09	0.66±0.65	0.65±0.07	0.38±0.03	0.57±0.06	NT	NT
12c	0.46±0.31	0.61±0.07	0.84±0.09	0.48±0.04	0.29±0.04	0.33±0.02	0.63±0.03	1.07±0.06
12d	0.88±0.40	0.57±0.48	0.43±0.05	1.22±0.65	0.57±0.06	0.74±0.03	NT	NT
12e	>10	>10	0.89±0.32	>10	0.80±0.02	>10	NT	NT
12f	>10	>10	5.62±1.76	>10	>10	>10	NT	NT
12g	>10	>10	6.46±1.11	>10	>10	>10	NT	NT
D	5.95±0.32	1.86±0.14	9.85±0.53	3.46±0.27	7.92±0.46	NT	NT	NT
5-FU	2.51±0.96	4.42±1.01	5.49±1.30	4.25±0.98	4.59±1.22	7.44±1.45	26.10±1.48	18.09±1.86

NT: not tested.

Effect of 16c on cell cycle and cell apoptosis

In order to investigate whether the cytotoxicity of **12c** was due to the cell cycle arrest, we evaluated the effect of compound **12c** on tumor cell cycle and apoptosis by flow cytometry method. The experimental result was shown in Figures 4 and 5. Additionally, when the concentration was 0.016 μM,

the proportions of G1 phase, S phase and G2 phase were 33.65%, 38.01% and 28.34%, respectively. Gradually, when the concentration rose to 0.4 μM, the ratio of G1 phase decreased to 15.95%, S phase decreased to 28.64%, G2 phase increased to 55.42%. And the percentage of total apoptosis cells, including Annexin V+/PI- (early apoptosis cells) and Annexin V+/PI- (late apoptosis and necrosis cells) increased from 11.15% to 61.14%. These results suggest that **12c** could exert antitumor effects through triggering the cell apoptosis.

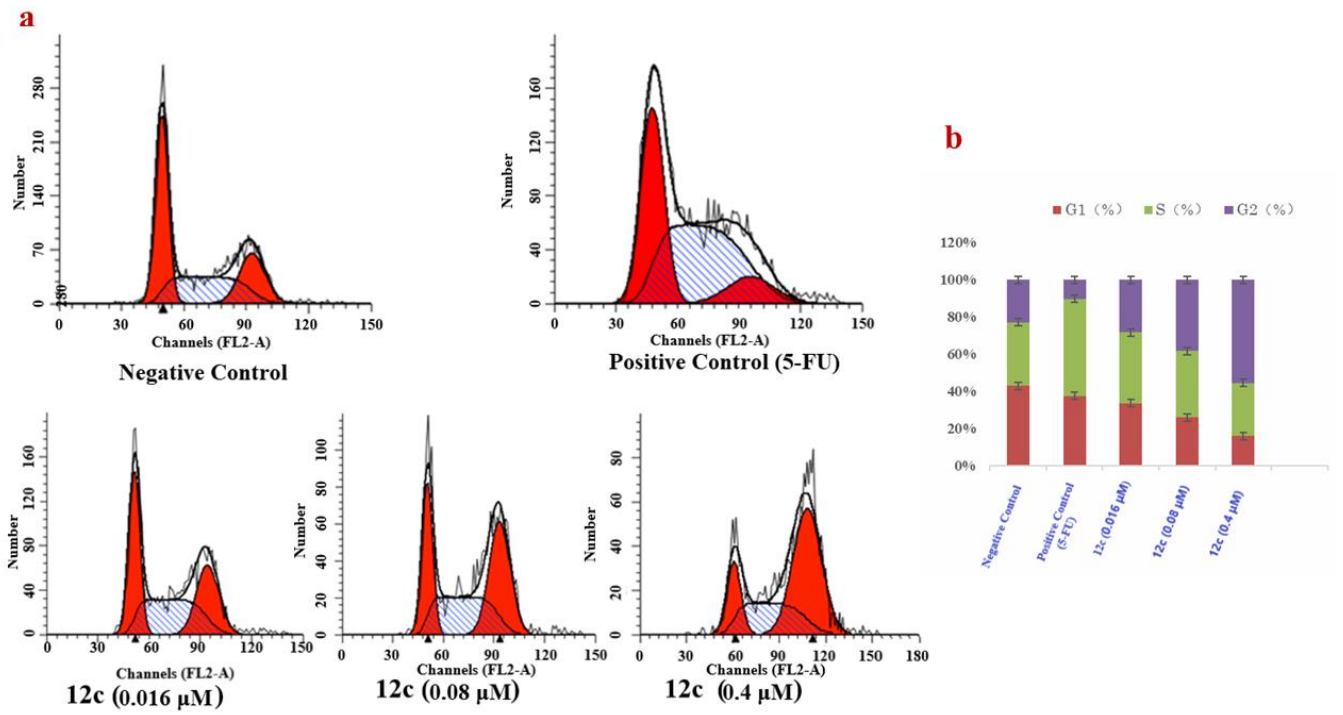

Figure 4. Effect of compound **12c** on the cycle of Bel-7402. Bel-7402 cells were exposed to various concentrations (0.016 - 0.4 μM) of **12c** in 72 h, and the cells were harvested and flow cytometry analyzed for cell cycle distribution by propidium iodide (PI) staining. (B) Distribution of the various phases of the cell cycle in Bel-7402 cells. The experiment was repeated three.

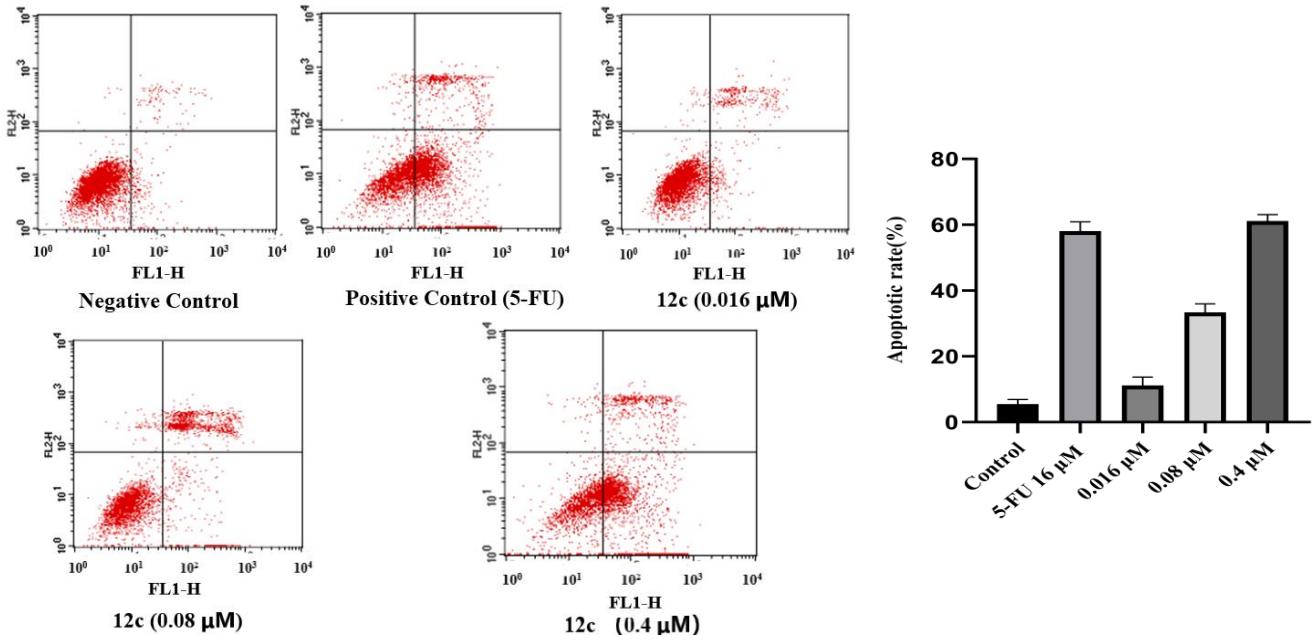

Figure 5. Compound **12c** induces Bel-7402 cell apoptosis. Bel-7402 cells were treated with DMSO or **12c** at various concentration for 72 h and the frequency of Bel-7402 apoptosis was determined by Annexin V+/PI staining and flow cytometry analysis.

Anti-tumor activity of 12c *in vivo*

In order to further evaluate the effect on cancer and safety of compound **12c** *in vivo*, the orthotopic Bel-7402/5-FU tumor-bearing nude mice were used to evaluate the anti-tumor efficiency. The mice were randomly divided into five groups (n = 6) and treated with **12c** at 50 mg/kg, 100 mg/kg dose oral daily. In addition, another group was treated with **12c** at 100 mg/kg by intraperitoneal injection. The positive control group was treated with 5-FU at 10 mg/kg by intraperitoneal injection. Mice treated with vehicle control showed significant tumor growth, reaching average volumes of 1334 mm^3 (Figure 6b). In comparison, three different treatment groups showed varying degrees of tumor growth inhibition. The anti-tumor effect of 100 mg/kg of compound **12c** was comparable with 5-FU at 10 mg/kg. Furthermore, the gross appearance of tumors (Figure 6b) and the tumor weights (Figure 6c) were consistent with the tumor volume. The inhibition ratio of tumor by **12c** at 50 mg/kg (p.o.), at 100 mg/kg (p.o.), 100 mg/kg (i.p.) and 5- Fu at 10 mg/kg (i.p.) were 43.33%, 51.64%, 61.36% and 19.91% when compared with the vehicle control at the end of the study, respectively. These results showed that compound **12c** exhibited an excellent inhibitory effect on tumor growth and the tumor growth inhibition (TGI) value was 61.36% with a dosage of 100 mg/kg/day (i.p.).

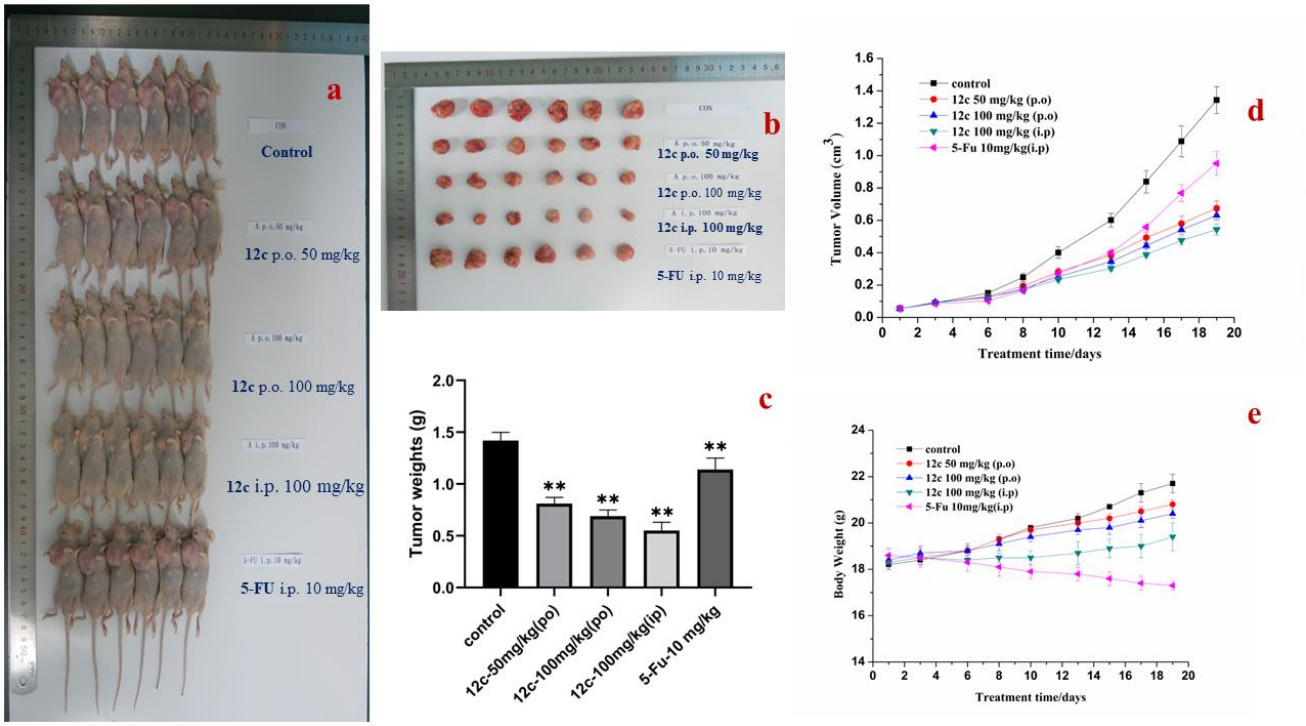

Figure 6. (a) Tumor volume of each mouse in the groups treated with control; **12c** at 50 mg/kg; **12c** at 100 mg/kg; **12c** at 100 mg/kg at i.p.; 5-Fu at 10 mg/kg at i.p.; (b) average tumor volumes and Image of isolated tumors; (c) average weights of tumors; body weights change of all four five groups; (d) Tumor volume of the mice in each group during the observation period. (e) Body weight of the mice from each group at the end of the observation period. The significant differences have been indicated, and ** represent $p < 0.01$, respectively.

Effect of compound 12c on apoptosis-related proteins

To further explore the anti-tumor molecular mechanism of **12c** *in vivo*, we examined the expression of Bcl-2, Bax, caspase-3 and H2AXp139 in xenografted tumor samples. As shown in Figure 6, Western blotting analysis exhibited that **12c** significantly up-regulated the expression of proapoptotic protein Bax, while down-regulated the expression of the antiapoptotic protein Bcl-2 in a dose dependent manner. Meanwhile, **12c** could also up-regulate the expression caspase-3 and the phosphorylation levels of H2AXp139. Caspase-3 is the most important terminal cleavage enzyme in the process of apoptosis. H2AX phosphorylation is related to tumor development. It is a critical executioner of apoptosis, and its activation requires the proteolytic processing of its inactive zymogen into activated cleaved caspase-3. The results suggest the antitumor mechanisms of **12c** could relate to DNA damage repair or apoptosis induction due to caspase-3 and H2AXp139 gene expression enhancement.

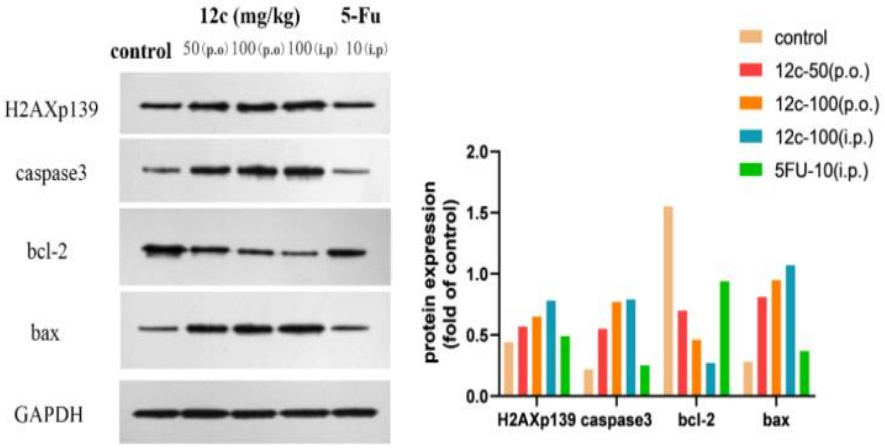

Figure 7. Western blotting of tumor tissue lysates to determine expressions angiogenesis-related proteins expression of Bcl-2, Bax, H2AXp139 and caspase3 proteins in tumors and quantitation of protein expression. Whole-cell lysates from control-untreated and treated tumors were analyzed by western blotting for protein expressions. GAPDH was measured as a loading control. There are five Lanes, which are Lane 1 (control), Lane 2 (**12c** 50 mg/kg/day/p.o.), Lane 3 (**12c** 100 mg/kg/day/p.o.), Lane 4 (**12c** 100 mg/kg/day/i.p.) and Lane 5 (5-FU 10 mg/kg/day/i.p.), respectively.

In summary, we successfully synthesized a series of coumarin derivatives **12a-g** and their structures were characterized by IR, HRMS and ^{1}H NMR. In addition, their inhibitory effects on human cancer cell lines HeLa, SW620, HepG-2, Bel-7402, HCT-116, MCF-7 and Bel-7402/5-FU lines were evaluated by MTT. As a result, it was found that most of these compounds exhibited significant inhibitory activities. It is notable that **12c** displayed the broad spectrum anti-proliferative effects *in vitro*. What is more, **12c** could effectively inhibit liver cancer growth when tested using a human hepatocellular carcinoma cell Bel-7402/5-FU xenograft model. In a word, compound **12c** is worth further investigating as an effective anticancer candidate.

EXPERIMENTAL

Melting points were measured using a WRS-1B melting point apparatus without any correction. ^{1}H NMR spectral data were recorded on Bruker Avance DPX400 and using TMS as an internal standard. Mass spectra were recorded on Thermo Fisher LTQ Orbitrap XL Liquid chromatography-mass spectrometry instrument.

Experimental procedures and product characterization

The following compounds have been already described in the literature: **5a~g**,[26] **11**.[25]

General procedure of synthesis of compounds 6a~g

Compounds **5a~m** (1.0 mmol, 1.0 equiv) and NaOH (3.0 mmol, 3.0 equiv) were added in 50% EtOH (20 mL) and stirred over 1 h at a temperature below 90 ℃. The reaction mixture was acidified with HCl (6 mol/L) until pH 1 and concentrated in a vacuum to afford crude products **6a~m** as a buff solid, then put in further reaction without purification.

General procedure of synthesis of target compounds 12a~g

Compounds **6a~g** (0.12 mmol, 1.2 equiv), compound **11** (310 mg, 1.0 mmol), DMAP (61 mg, 0.05 mmol), EDCI (230 mg, 1.2 mmol), TBAB (380 mg, 0.12 mmol) were dissolved in DCM (15 mL) and stirred at room temperature over 24 h. The reaction mixture was dumped into 100 mL H_2O and extracted with DCM (3 × 15 mL) and washed with saturated aqueous $NaHCO_3$ (2 × 15 mL) and brine. The organic layer was dried with anhydrous Na_2SO_4 and concentrated in a vacuum to afford buff or orange oil which was passed through a column of silica gel with MeOH / CH_2Cl_2 (1:30). The solvent was removed under vacuum and the target compounds **12a~g** were obtained.

4-((4-((7-(2-Morpholinoethoxy)-2-oxo-2*H*-chromene-3-carbonyl)oxy)but-2-yn-1-yl)oxy)-3-(phenylsulfonyl)-1,2,5-oxadiazole 2-oxide (12a)

Orange solid; yield: 65.5%; mp 151.2.1-152.3 ℃; IR (KBr, cm^{-1}) *υ*: 3410, 1756, 1628, 1613, 1557, 1358, 1206, 1164, 1114, 1024, 938; ^{1}H NMR (400 MHz, Chloroform-*d*) δ 8.57 (s, 1H, ArH), 8.07 (d, *J* = 7.4 Hz, 2H, ArH), 7.76 (t, *J* = 7.5 Hz, 1H, ArH), 7.64 (t, *J* = 7.8 Hz, 2H, ArH), 7.53 (d, *J* = 8.7 Hz, 1H, ArH), 6.91 (d, *J* = 8.8 Hz, 1H, ArH), 6.82 (d, *J* = 2.2 Hz, 1H, ArH), 5.11 (s, 2H, OCH_2), 4.98 (s, 2H, OCH_2), 4.22 (t, *J* = 5.5 Hz, 2H, OCH_2), 3.75 (t, *J* = 4.7 Hz, 4H, Morpholine), 2.87 (t, *J* = 5.6 Hz, 2H, NCH_2), 2.61 (t, *J* = 4.6 Hz, 4H, Morpholine). HRMS (*m/z*): $[M+H]^+$ calculated for 612.1288; found, 612.1292.

4-((4-((7-(3-Morpholinopropoxy)-2-oxo-2*H*-chromene-3-carbonyl)oxy)but-2-yn-1-yl)oxy)-3-(phenylsulfonyl)-1,2,5-oxadiazole 2-oxide (12b)

Orange solid; yield 66.4%; mp 193.3-194.0 ℃; IR (KBr, cm^{-1}) *υ*: 3419, 1768, 1616, 1557, 1360, 1292, 1212, 1167, 1111, 602. ^{1}H NMR (600 MHz, DMSO-d_6) δ 8.73 (s, 1H, ArH), 8.01 (d, *J* = 7.8 Hz, 2H, ArH), 7.88 – 7.81 (m, 2H, ArH), 7.73 (t, *J* = 7.8 Hz, 2H, ArH), 7.04 – 6.98 (m, 2H, ArH), 5.27 (s, 2H, OCH_2), 5.06 (s, 2H, OCH_2), 4.16 (t, *J* = 6.3 Hz, 2H, OCH_2), 3.56 (t, *J* = 4.8 Hz, 4H, Morpholine), 2.43 – 2.33 (m, 6H, Morpholine, NCH_2), 1.83 – 1.79 (m, 2H, CH_2CH_2). HRMS (*m/z*): $[M+H]^+$ calculated for 626.1445; found, 626.1421.

4-((4-((7-(4-Morpholinobutoxy)-2-oxo-2*H*-chromene-3-carbonyl)oxy)but-2-yn-1-yl)oxy)-3-(phenylsulfonyl)-1,2,5-oxadiazole 2-oxide (12c)

Orange solid, yield 68.1%, mp 109.7-110.1 ℃; IR (KBr, cm^{-1}) *υ*: 3413, 2955, 1768, 1610, 1554, 1465, 1387, 1360, 1292, 1203, 1167, 1114, 608; ^{1}H NMR (400 MHz, Chloroform-*d*) δ 8.57 (s, 1H, ArH), 8.07 (d, *J* = 7.3 Hz, 2H, ArH), 7.76 (t, *J* = 7.5 Hz, 1H, ArH), 7.64 (t, *J* = 7.9 Hz, 2H, ArH), 7.52 (d, *J* = 8.7 Hz, 1H, ArH), 6.88 (d, *J* = 8.8 Hz, 1H, ArH), 6.79 (d, *J* = 2.3 Hz, 1H, ArH), 5.11 (s,

2H, OCH_2), 4.98 (s, 2H, OCH_2), 4.09 (d, *J* = 6.3 Hz, 2H, OCH_2), 3.72 (t, *J* = 4.7 Hz, 4H, Morpholine), 2.51 – 2.43 (m, 6H, Morpholine, NCH_2), 1.90 – 1.84 (m, 2H, CH_2CH_2), 1.73 – 1.67 (m, 2H, CH_2CH_2). HRMS (*m/z*): $[M+H]^+$calculated for 640.1601; found, 640.1585.

4-((4-((7-((5-Morpholinopentyl)oxy)-2-oxo-2*H*-chromene-3-carbonyl)oxy)but-2-yn-1-yl)oxy)-3-(phenylsulfonyl)-1,2,5-oxadiazole 2-oxide (12d)

Orange solid; yield 69.7%; mp 125.7-127.8 ℃; IR (KBr, cm^{-1}) υ: 3425, 2937, 2857, 1777, 1616, 1557, 1381, 1363, 1206, 1170, 1111, 602; ^{1}H NMR (400 MHz, DMSO-d_6) δ 8.80 (s, 1H, ArH), 8.02 (d, *J* = 7.4 Hz, 2H, ArH), 7.89 – 7.85 (m, 2H, ArH), 7.76 (d, *J* = 7.9 Hz, 2H, ArH), 7.04 – 6.99 (m, 2H, ArH), 5.28 (s, 2H, OCH_2), 5.06 (s, 2H, OCH_2), 4.13 (d, *J* = 6.4 Hz, 2H, OCH_2), 3.55 (t, *J* = 4.7 Hz, 4H, Morpholine), 2.34 – 2.26 (m, 6H, Morpholine, NCH_2), 1.77 – 1.73 (m, 2H, CH_2CH_2), 1.49 – 1.41 (m, 4H, CH_2CH_2). HRMS (*m/z*): $[M+H]^+$ calculated for 654.1758; found, 654.1749.

4-((4-((7-((6-Morpholinohexyl)oxy)-2-oxo-2*H*-chromene-3-carbonyl)oxy)but-2-yn-1-yl)oxy)-3-(phenylsulfonyl)-1,2,5-oxadiazole 2-oxide (12e)

Orange solid; yield 71.2%; mp 135.7-138.5 ℃; IR (KBr, cm^{-1}) *υ*: 3428, 2940, 1777, 1622, 1557, 1465, 1450, 1358, 1206, 1164, 1117, 605; ^{1}H NMR (400 MHz, DMSO-d_6) δ 8.80 (s, 1H, ArH), 8.02 (d, *J* = 7.8 Hz, 2H, ArH), 7.89 – 7.85 (m, 2H, ArH), 7.75 (t, *J* = 7.7 Hz, 2H, ArH), 7.05 – 6.98 (m, 2H, ArH), 5.28 (s, 2H, OCH_2), 5.06 (s, 2H, OCH_2), 4.12 (t, *J* = 6.5 Hz, 2H, OCH_2), 3.54 (t, *J* = 4.7 Hz, 4H, Morpholine), 2.34 – 2.21 (m, 6H, Morpholine, NCH_2), 1.77 – 1.70 (m, 2H, CH_2CH_2), 1.47 – 1.39 (m, 4H, CH_2CH_2), 2.36 – 2.30 (m, 2H, CH_2CH_2). HRMS (*m/z*): $[M+H]^+$ calculated for 668.1914; found, 668.1905.

4-((4-((7-(3-(Diethylamino)propoxy)-2-oxo-2*H*-chromene-3-carbonyl)oxy)but-2-yn-1-yl)oxy)-3-(phenylsulfonyl)-1,2,5-oxadiazole 2-oxide (12f)

Orange solid; yield 65.8%; mp 110.7-112.9 ℃; IR (KBr, cm^{-1}) *υ*: 3416, 2940, 2857, 1768, 1610, 1548, 1447, 1360, 1292, 1206, 795, 596; ^{1}H NMR (600 MHz, DMSO-d_6) δ 8.70 (s, 1H, ArH), 7.98 (d, *J* = 7.8 Hz, 2H, ArH), 7.85 – 7.78 (m, 2H, ArH), 7.70 (t, *J* = 7.8 Hz, 2H, ArH), 7.01 – 6.93 (m, 2H, ArH), 5.24 (s, 2H, OCH_2), 5.07 (s, 2H, OCH_2), 4.13 (t, *J* = 6.3 Hz, 2H, OCH_2), 2.40 – 2.31 (m, 6H, NCH_2), 1.78 (m, 2H, CH_2CH_2), 1.29 – 1.16 (t, *J* = 7.8 Hz, 3H, CH_2CH_3), 1.07 – 0.98 (t, *J* = 7.9 Hz, 3H, CH_2CH_3). HRMS (*m/z*): $[M+H]^+$ calculated for 612.1652; found, 612.1645.

4-((4-((7-(4-(Diethylamino)butoxy)-2-oxo-2*H*-chromene-3-carbonyl)oxy)but-2-yn-1-yl)oxy)-3-(phenylsulfonyl)-1,2,5-oxadiazole 2-oxide (12g)

Orange solid; yield 65.9%; mp 90.9-92.0 ℃; IR (KBr, cm^{-1}) *υ*: 3419, 2931, 2848, 1759, 1718, 1616, 1551, 1447, 1360, 1209, 1167, 1027, 998, 792, 599; ^{1}H NMR (400 MHz, Chloroform-*d*) δ 8.58 (s, 1H, ArH), 8.06 (d, *J* = 7.4 Hz, 2H, ArH), 7.78 (t, *J* = 6.9 Hz, 1H, ArH), 7.65 (t, *J* = 7.9 Hz, 2H, ArH), 7.54 (d, *J* = 8.7 Hz, 1H, ArH), 6.90 (dd, *J* = 8.8, 2.3 Hz, 1H, ArH), 6.81 (d, *J* = 2.4 Hz, 1H, ArH),

5.13 (s, 2H, OCH_2), 5.00 (s, 2H, OCH_2), 4.11 (t, J = 6.3 Hz, 2H, OCH_2), 2.48 (m, 6H, NCH_2), 1.92 – 1.86 (m, 2H, CH_2CH_2), 1.74 – 1.69 (m, 2H, CH_2CH_2), 1.27 – 1.24 (t, J = 8.0 Hz, 3H, CH_2CH_3), 1.07 – 1.03 (t, J = 8.1 Hz, 3H, CH_2CH_3). ESI-MS (*m/z*): $[M+H]^+$ calculated for 626.1808; found, 626.1799.

The solubility test

Approximately 1 mg of the test compounds **12a-g** is dissolved in 10 mL MeOH, respectively. This solution is shaken for 5 h until completely dissolved. Then the maximum absorption wavelength of each compound was determined using UV. Subsequently, they were divided and diluted into 5 kinds of different concentrations solutions, respectively. The absorbance value of **12a-g** was measured under the maximum absorption wavelength, and the standard concentration-absorption curve of each compound was confirmed. To weigh an appropriate amount of these test compounds, then adding 5 mL water and stirring for 5 h at room temperature, their saturated solution was obtained by micro-aperture filter membrane, respectively. The absorbance value of **12a-g** was measured using UV, and their solubility was obtained by standard curve, respectively. The cLogP was calculated by software SYBYL-X 2.1.1.

Anti-proliferation activity test

The anti-proliferation activity was assessed by using MTT method. Tumor cells were planted on 96-well plates with 5×10^4 per well and incubated for 24 h under 37 ℃ and 5% CO_2 and then exposed to test compound at different concentrations for 72 h. Then the MTT solution (5 mg / mL) was added 20 μL per well, and incubated for 4 h, and the OD value was recorded at 490 nm. The IC_{50} value was calculated by the logit method. Each concentration was measured 3 times in parallel.

Analysis of cells apoptosis

Bel-7402 cells were planted at 5×10^5 per well in a 6-well plate and incubated for 24 h and then exposed to test compound at different concentrations, and incubated for 48 h. Then the cells were harvested and washed in PBS buffer solution, and suspended by Binding buffer solution (500 μL), and mixed with Annexin V-APC solution (5 μL) then reacted for 5-15 min in a dark place before analysis.

Analysis of cells cycle

Bel-7402 cells were planted at 5×10^5 per well in a 6-well plate and incubated for 24 h and then exposed to test compound at different concentrations, and incubated for 72 h. Then the cells were harvested and washed in PBS buffer solution, and fixed in 70% EtOH for at least 2 h. After that, added RNase A (100 μL), and heated under 37 ℃ at least 30 min, and added propidium iodide solution (400 μL) reacted under 4 ℃ at least 30 min in the dark. The stained cells were analyzed by a flow cytometer.

***In vivo* anti-tumor effect**

Female BALB/c nude mice at 4-5 weeks of age were purchased from Shanghai Lingchang BioTech Co. Ltd. (Shanghai, China). The mice were inoculated subcutaneously with 7402 / FU cells (1×10^7 suspended

in 1 mL of PBS for each mouse). The mice were divided into five groups (n = 6) randomly. When the tumor volume reached around 50-75 mm^2, mice were respectively treated with vehicle control, **12c** at 50 mg/kg, **12c** at 100 mg/kg by p.o every day, and 5-Fu group was treated with 5-Fu at 10 mg/kg by intra peritoneal injection every day. The vehicle control group only received an injection of the same amount of saline by intra peritoneal injection every day. Administration of vehicle or compound and monitoring tumor progression were done once every 2 days. While body weight and tumor volumes were measured and recorded every 2 days. After 21 days, the mice were weighed and sacrificed, and their tumors were dissected out and weighed.

Western Blot Analysis of xenograft 7402/FU tumors

To take the tumors tissue above the different groups, these tissues were cut, washed with cold 1× PBS, and lysed with RIPA lysis buffer (Beyotime, China) for 30 min on ice, then centrifuged at 12000 g for 15 min at 4 °C. The total protein concentration was determined by BCA protein assay kit (Beyotime, China). Equal amounts (30 μg per load) of protein samples were subjected to SDS−PAGE electrophoresis and transferred onto polyvinylidene fluoride (PVDF PBST) membranes (Millipore) which were then blocked in 10% nonfat milk (BD Biosciences) and reacted with primary antibodies. The antibodies against Bcl-2, Bax, caspase-3, H2AXp (Ser139) were purchased from Santa Cruz Biotechnology, and β-actin were purchased from Cell Signaling Technology. The protein bands were developed by the chemiluminescent reagents (Millipore). The densitometric analysis of the bands was performed by using the program ImageJ v1.33u.

Statistical analysis

All data were presented as mean ± standard deviation (SD). Statistical significance was performed by two-tailed Student's t-tests for two groups and one-way SPSS (Statistic Package for the Social Science) 17.0 for multiple groups, and $p < 0.05$, $p < 0.01$ were considered as a significant difference (remarked with *, **, and ***, respectively). All data were processed by SPSS (Staffstical Package for the Social Science) 17.0.

ACKNOWLEDGEMENTS

This work is thanks to the great support of the National Natural Science Foundation of China (No.KJ2017A292).

REFERENCES

1. H. Sung, J. Ferlay, R. L. Siegel, M. Laversanne, I. Soerjomataram, A. Jemal, and F. Bray, *CA Cancer J. Clin*., 2021, **71**, 209.
2. R. Qun, Y. E. Moussa, and N. J. Wheate, *Dalton Trans*., 2018, **47**, 6645.

3. T. Iwamoto, *Biol. Pharm. Bull*., 2013, **36**, 715.
4. S. Dhawan, N. Kerru, P. Awolade, A. Singh-Pillay, S. T. Saha, M. Kaur, S. B. Jonnalagadda, and P. Singh, *Bioorg. Med. Chem.*, 2018, **26**, 5612.
5. S. A. T. Fobofou, K. Franke, W. Brandt, A. Manzin, S. Madeddu, G. Serreli, G. Sanna, and L. A. Wessjohann, *Nat. Prod. Res.*, 2023, **37**, 1947.
6. B. M. Chougala, S. Samundeeswari, M. Holiyachi, N. S. Naik, L. A. Shastri, S. Dodamani, S. Jalalpure, S. R. Dixit, S. D. Joshi, and V. A. Sunagar, *Eur. J. Med. Chem*., 2018, **143**, 1744.
7. S. A. L. Madeiro, N. H. P. B. Borges, A. L. Souto, P. T. R. De-Figueiredo, J. P. Siqueira-Junior, and J. F. Tavares, *Microb. Pathog.*, 2017, **104**, 151.
8. K. Skalicka-Woźniak, I. E. Orhan, G. A. Cordell, S. M. Nabavi, and B. Budzyńska, *Pharmacol. Res.*, 2016, **103**, 188.
9. F. V. Fonseca, L. Baldissera Jr., E. A. Camargo, E. B. S. Diz-Filho, A. G. Correa, L. O. Beriam, D. O. Toyama, C. A. Cotrim, J. Alvin Jr., and M. H. Toyama, *Toxicon*, 2010, **55**, 1527.
10. D. N. Patagar, R. Kusanur, S. R. Batakurki, S. M. Patra, N. R. Patil, and J. H. Patil, *J. Mol. Struct*., 2023, **1294**, 136377.
11. E. Ortega-Forte, A. Rovira, A. Gandioso, J. Bonelli, M. Bosch, J. Ruiz, and V. Marchan, *J. Med. Chem*., 2021, **64**, 17209.
12. G. S. Lingaraju, K. S. Balaji, S. Jayarama, S. M. Anil, K. R. Kiran, and M. P. Sadashiva, *Bioorg. Med. Chem. Lett.*, 2018, **28**, 3606.
13. E. Y. Ahmed, N. A. A. Latif, M. F. El-Mansy, W. S. Elserwy, and O. M. Abdelhafez, *Bioorg. Med. Chem. Lett.*, 2020, **28**, 115328.
14. T. Nasr, S. Bondock, and M. Youns, *Eur. J. Med. Chem.*, 2014, **76**, 539.
15. K. M. Amin, A. A. M. Eissa, S. M. Abou-Seri, F. M. Awadallah, and G. S. Hassan, *Eur. J. Med. Chem*., 2013, **60**, 187.
16. L. R. Zhang, G. R. Jiang, F. Yao, Y. He, G. Q. Liang, Y. S. Zhang, B. Hu, Y. Wu, Y. S. Li, and H. Y. Liu, *PLOS ONE*, 2012, **7**, e37865.
17. S. H. Wu, Z. H. Zhang, and J. B. Zhao, *China J. Chin. Mater. Med.*, 1998, **2**, 303.
18. T. Yamamoto, T. Nakayama, J. Yamaguchi, M. Matsuzawa, M. Mishina, K. Ikeda, and H. Yamamoto, *Neurosci. Lett.*, 2016, **610**, 48.
19. K. J. A. Mccullagh, R. Cooney, and T. O'Brien, *Nitric Oxide*, 2016, **30**, 41.
20. C. Moore, D. Sanz-Rosa, and M. Emerson, *Eur. J. Pharm.*, 2011, **651**, 152.
21. A. A. Timoshin, V. L. Lakomkin, A. A. Abramov. E. K. Ruuge, V. I. Kapel'ko, E. I. Chazov, and A. F. Vanin, *Eur. J. Pharm.*, 2015, **765**, 525.
22. T. Kubo, H. Nakajima, M. Nakatsuji, M. Itakura, A. Kaneshige, Y. T. Azuma, T. Inui, and T. Takeuchi,

Nitric Oxide, 2016, **53**, 13.

23. K. Kashfi and B. Rigas, *Biochem. Biophys. Res. Commun.*, 2007, **358**, 1096.
24. M. M. Liu, X. Y. Chen, Y. Q. Huang, P. Feng, Y. L. Guo, G. Yang, and Y. Chen, *J. Med. Chem.*, 2014, **57**, 9343.
25. Z. Zhang, Z. W. Bai, Y. Ling, L. Q. He, P. Huang, H. X. Gu, and R. F. Hu, *Med. Chem. Res.*, 2018, **27**, 1198.
26. J. K. Huang, Z. Zhang, P. Huang, L. Q. He, and Y. Ling, *Med. Chem. Commun*., 2016, **7**, 1812.